

On Extreme Value Properties of Vertical Bending Moment

Themistoklis Sapsis,¹ Vlasdas Pipiras,² Kenneth Weems,³ and Vadim Belenky³

(¹Massachusetts Institute of Technology,

²University of North Carolina at Chapel Hill,

³David Taylor Model Basin / NSWCCD, USA)

ABSTRACT

The paper describes a study of the properties of extreme values of wave induced vertical bending moment (VBM) for a ship in irregular head seas. The objective of this study is to formulate a physics-informed model of extreme vertical bending moment for the evaluation of lifetime loads.

The numerical part of the study involves the use of a nonlinear, time-domain seakeeping code to generate large (5,000 hour) sets of VBM data in random head waves. These data sets reveal the shape of the tail of the distribution of VBM and outline the principle nonlinearities of the problem. It is demonstrated that the inclusion of water pressure on the foredeck of the ship significantly changes the tail shape in high sea states. It is also shown that the common practice of fitting a Weibull distribution to the peaks of the VBM data does not properly represent the extreme VBM values from simulations that include the effect of water on deck.

The analytical part of the study includes the formulation of a “volume-based” reduced order model for VBM, based on the computation of submerged volumes of a series of hull sections. Irregular wave responses are modeled with two components of random amplitudes, with the wave length of both of them equal to ship length, and allows the distribution of VBM to be computed directly. The model reflects the wave influence on the vertical bending moment and compares well with the numerical simulation results that do not include pressures on deck.

INTRODUCTION

The topic of this paper is the classic extreme value properties of the wave-induced vertical bending moment, which has been a subject of interest since the introduction of spectrum-based irregular waves in naval architecture by St. Denis and Pierson (1953). The application of the Weibull distribution to compute lifetime extreme wave-induced loads has been a standard engineering method, probably since the 1960s. The application of extreme value theory to the calculation of wave-induced loads was

considered by Ochi and Wang (1976) and further described in Ochi (1981). The present work attempts to develop a physics-informed model that could provide an accurate statistical extrapolation from a small volume of simulation or model test data.

Belenky *et al.* (2018) describes the application of physics-informed statistical extrapolation of roll motion data to predict the probability of extreme roll angle and capsizing. The “enabling technology” for this application is a qualitatively-correct reduced-order motion model that allows analytical or even closed form solution for extreme values. This solution reveals a structure of the distribution tail and allows the use of a particular model for the tail. The fitting of the tail is therefore no longer driven only by the data – some physical considerations are also included into the statistical model. A data perspective of this approach for VBM is given by Brown and Pipiras (2020).

A single degree-of-freedom (DOF) dynamical system with piecewise linear stiffness was used as a reduced-order mathematical model for roll motion and capsizing. The model is qualitatively correct, as it reproduces the topology of the phase plane. Piecewise linear stiffness allows the derivation of a closed-form expression for the peaks of roll motion. Then the distribution of roll peaks can also be derived in analytical form. It was found that the tail of the roll peak distribution has a complex structure: a heavy tail from the vicinity of the maximum of the roll restoring (GZ) curve, which then becomes light and has an upper bound near the angle of vanishing stability (Belenky *et al.* 2019).

The 1-DOF roll model with piecewise linear stiffness has been shown to exhibit the principal known behavior of nonlinear ship roll motion (Belenky 2000). Thus, the shape of the distribution tail from the piecewise linear system can be extended to ship rolling motion from more advanced 3-DOF and 6 DOF models. A Pareto distribution is used to model the heavy tail, leading to an extrapolation of reasonable statistical uncertainty from a modest volume of time-domain data (Belenky *et al.* 2018). Limited validation results are also available from the cited reference.

SIMULATIONS AND OBSERVATIONS

For a reduced-order model to be useful, it must be able to capture the principal characteristics and nonlinearities of the modeled process. The main nonlinear factor for ship roll motions is known to be the variable stiffness represented by the GZ curve. What is the main nonlinear factor for wave-induced vertical bending moment that has to be reflected in a reduced-order model?

To answer this question, a set of 5,000 hour irregular seas simulations were carried out. The ship configuration was the flared variant of the ONR Topsides Hull Series (Bishop *et al.* 2005). This is a companion model to the often-studied ONR Tumblehome hull form, but with a topsides shape more typical of conventional naval surface combatants of the last 30 years. The geometry of the ship is shown in Figure 1.

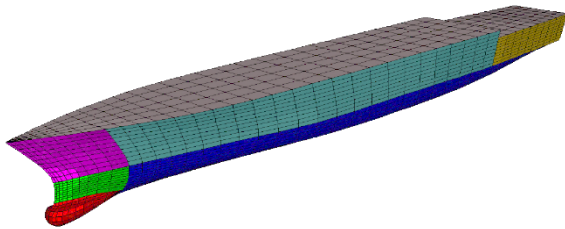


Figure 1: Geometry of ONR Topsides series flared hull

Simulations were performed using the Large Amplitude Motion Program (LAMP), which is a time-domain ship motions and wave loads simulation code incorporating a body-nonlinear calculation of the incident wave (Froude-Krylov) and hydrostatic restoring pressure forces and a 3-D potential flow panel solution of the wave-body disturbance (Shin *et al.* 2003). LAMP computes a pressure distribution on the wetted portion of the hull surface at each time increment, which is integrated to get the forces acting on the hull. Once forces are available, the 6-DOF equations of motion are solved for the next step.

The main girder loads, including VBM, are computed by modeling the hull as a rigid beam and performing a partial integration of the pressure to each side of the specified load calculation planes. A longitudinal distribution of the ship's mass is used to account for weight and inertial forces in the sectional load calculations. The LAMP System includes an elastic beam model for slam-induced whipping loads (Weems *et al.* 1998), but the present analysis considers only the wave frequency loads.

In the calculation of motions and loads, there are several options for handling the deck of the ship in situations where the relative motion is such that the deck might enter the water, or water might flow onto the deck. The simplest option is a “no-deck” approach that ignores any water on the deck. This approach effectively assumes that the deck stays dry regardless of its motion relative to the wave surface, and it results in an ever increasing pitch

restoring moment and VBM as the bow is submerged in a wave.

A second, and nearly as simple, option for handling the deck is to include it in the wave-body interaction problem in the same fashion as the ship hull. This can be considered to be a “deck-in-water” approach. In LAMP's approximate body-nonlinear approach, this consists of including the body-nonlinear Froude-Krylov and hydrostatic pressure over the deck surface but neglecting the disturbance potential, which is computed over the mean wetted hull surface. In this approach, the deck is effectively assumed to become instantly wet when the relative motion of the ship causes it to be submerged below the incident wave surface. With this calculation of the deck pressure, the pitch restoring moment and VBM become “capped” as the bow is submerged in a wave.

A third, but considerably more complicated, option is to use a “green-water-on-deck” model. This attempts to compute the flow over the deck based on the relative wave elevation at the deck edge and the motions of the ship (Belenky *et al.* 2003). Green-water-on-deck models range from a simple, empirical formula for the depth of the water on the deck based on the relative motion at the deck edge to full numerical simulations of the flow over the deck. The latter models can provide a more realistic estimate of water-on-deck effects, including the latency in the ingress and egress of green-water, but with considerable additional complexity and cost. LAMP includes a green-water-on-deck model incorporating a coupled shallow-water finite-volume numerical solution of the flow over the deck (Liut *et al.* 2013).

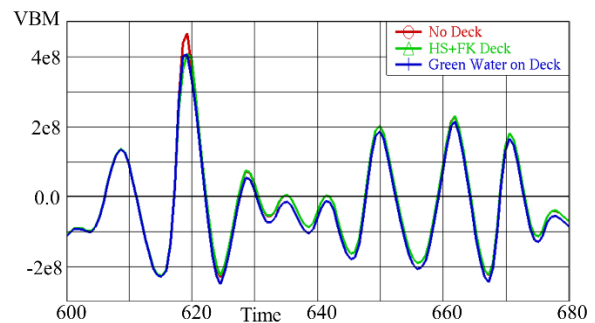


Figure 2: Effect of deck pressure option on VBM

Figure 2 illustrates the effect of the deck pressure option during a relatively small water-on-deck event in moderate sea conditions (head sea state 6, 10 knots). The red curve shows the no-deck result, which has the largest peak VBM (+ is sagging, - is hogging). The green curve shows the deck-in-water result with hydrostatic and Froude-Krylov pressure on the deck, with a reduction in the peak VBM. The blue curve shows the result with the numerical solution of green-water-on-deck, which shows a similar reduction in the peak VBM, but with a slight lag due to the latency

associated with the delayed ingress of water. Outside of the peak, the difference in the approach is minimal, though the numerical green-water-on-deck model does show some shift in the VBM due to residual water on deck. Figure 3 shows a close-up of the peak of the VBM curves. The deck option also affects the pitch motion, but the difference is insignificant in this case.

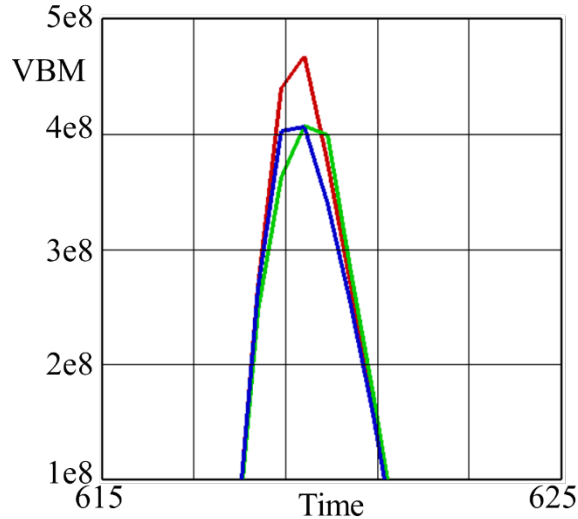


Figure 3: Effect of deck pressure option on VBM (close-up)

This example shows that the deck option can have a significant effect on the peak load values, even for moderate events. To explore the distribution of VBM, large simulation data sets were run for the flared hull running at 10 knots into Sea State 5 (SS5), where water on deck events are expected to be rare, and Sea State 7 (SS7), where water on deck events are expected to be frequent and severe. The SS7 cases were run without deck pressure and with the deck-in-water approach described above, while SS5 was run only with the deck-in-water approach. Problems with the robustness of the numerical green-water-on-deck model prevented it from being used in this simulation.

Table 1 Parameters of Numerical Simulation

Ship length, m	154
Ship breadth, m	18
Ship draft, m	5.5
KG, m	8.7
Speed, kt	10
Heading, deg	180
Number of frequencies	250
Length of record, s	1900
SS 7, significant wave height, m	7.62
SS 7, modal period, s	13.0
SS 5, significant wave height, m	4.0
SS 5, modal period, s	9.7

Details of the ship and simulation are given in Table 1. Each case was run as 10,000 independent records of just over 30 minutes duration each, providing 5,000 hours of data after eliminating transient effects. The seaway was modeled as long-crested head seas using a Bretschneider two-parameter spectrum, with 250 component frequencies to avoid self-repeat issues and different sets of pseudo-random phases to generate independent realizations of the waves.

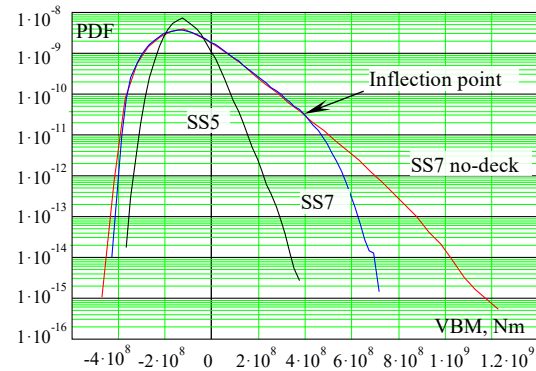


Figure 4: Histograms of instantaneous values of VBM amidships

Figure 4 shows a plot of histograms for the instantaneous value of the computed vertical bending moment at the midship section for all three sets. Sagging is considered to be positive for the VBM, while hogging is negative. There is an obvious difference between the histograms with and without deck pressure for SS7. The histograms lie on top of each other until about 4.5×10^8 Nm and then diverge. The no-deck continues almost as a straight line, while the deck-in-water case bends and drops much faster.

Inclusion of pressures on deck decreases the bending moment, as it limits the increase of buoyance force, while the weight component of the VBM remains the same. The deck-in-water histogram for SS7 has an obvious “inflection point,” after which the tail becomes lighter. Similar behavior has been observed in the tail of the distribution of roll motions near the angle of vanishing stability (Belenky *et al.* 2018, 2019).

No inflection point is observed in the SS5 results, despite the fact that the deck-in-water pressures were included in the calculations. The SS5 histogram has a tail structure similar the SS7 no-deck case. The water on deck seems to have little effect on VBM at SS5, likely because too small a portion of the deck gets wet and too rarely.

Hogging tails seem to be quite similar for all three cases. However, hogging does not represent practical interest in this study, as the extreme loads are dominated by sagging.

Figure 5 shows similar histograms computed for positive (sagging) peaks of the vertical bending

moment. The tails of the distribution follows the same pattern: presence of the inflection point on the SS7 with deck histogram, while no inflection point is observed for the SS5 results.

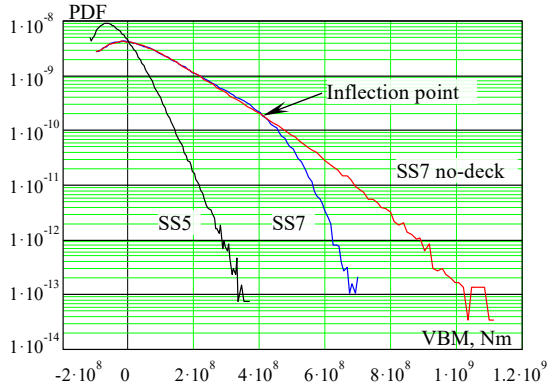


Figure 5: Histograms of positive peaks of VBM amidships

WEIBULL FITS FOR THE PEAKS

Standard procedures for the assessment of life-time extreme loads use a Weibull distribution fit to several hours of simulation results. The authors are not aware of any theoretical background for using Weibull distribution for extreme loads. However, practice of its application counts several decades and has been generally considered to be successful.

The probability density function (PDF) of the Weibull distribution for a random variable $x > u$ is expressed as:

$$PDF(x) = \frac{k}{\lambda} \left(\frac{x-u}{\lambda}\right)^{k-1} \exp\left(-\left(\frac{x-u}{\lambda}\right)^k\right) \quad (1)$$

where k is shape parameter, λ is scale parameter and u is a location parameter.

The standard technique for estimating the shape and scale parameters is the maximum likelihood estimator (MLE). Using formulae from Cohen (1965), the shape parameter is found from a single nonlinear algebraic equation:

$$\frac{1}{k} + \frac{1}{N} \sum_{i=1}^N \ln(y_i) - \frac{\sum_{i=1}^N y_i^k \ln(y_i)}{\sum_{i=1}^N y_i^k} = 0 \quad (2)$$

where $y_i = x_i - u$. The scale parameter is then computed as:

$$\hat{\lambda} = \left(\frac{1}{N} \sum_{i=1}^N y_i^k\right)^{\frac{1}{k}} \quad (3)$$

The location parameter is used when only part of the data is used for the fitting, so here $u = 0$.

Figure 6 shows a Weibull fit using 10 hours of simulation data for SS7 with the deck pressures included. Visually, the fit is good until a VBM value of about 4.5×10^8 Nm, which is close to the inflection point. Figure 7 shows two other cases: SS5 with deck-in-water

pressures and SS7 no-deck. Neither of these cases has an inflection point, and Weibull fits very well.

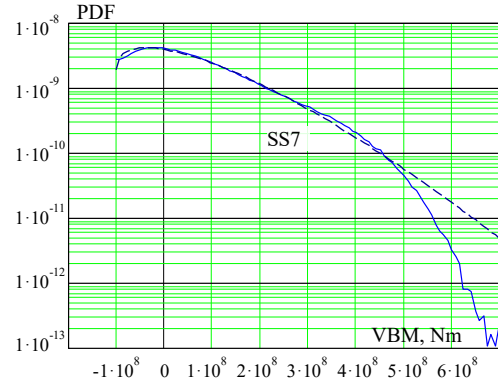


Figure 6: Weibull fit for positive peaks of VBM, SS7 deck-in-water pressure included.

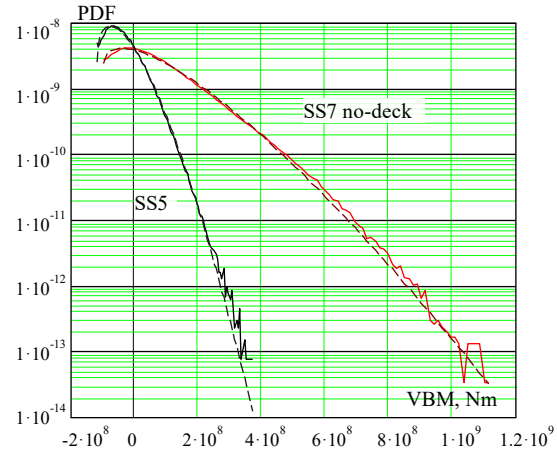


Figure 7: Weibull fit for positive peaks of VBM, SS7 and SS5

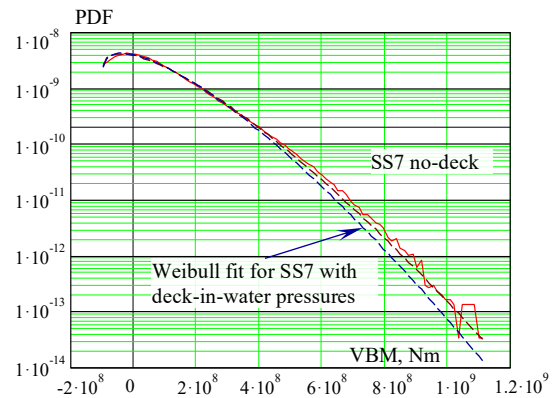


Figure 8: Comparison of Weibull fits for positive peaks of VBM, SS7

Figure 8 compares Weibull fits with and without deck pressure. The difference between these fits is small but noticeable. The difference is caused by the influence of deck pressure, making the blue tail slightly lighter. Obviously, the Weibull distribution does not properly fit the change in data beyond the inflection point. A similar conclusion was made by Brown and Pipiras (2020), where all the data was used for the fit.

The condition of the appearance and the location of the inflection point provides important practical information, as it indicates the applicability of the Weibull distribution.

VOLUME-BASED REDUCED-ORDER MODEL

To develop a reduced-order model of vertical bending moment in irregular waves, consider the area of submerged portion of a station at a ship location x , measured from the midship section:

$$A(x, \theta x + h(x, t))$$

where θ is the pitch angle and $h(x, t)$ is the wave elevation. It is natural to expect that the function A is monotonically increasing and therefore invertible with respect to its second argument.

The random waves around the ship are approximated as a white-noise, narrow-band stochastic process.

$$h(x, t; \zeta) = \alpha_c(t; \zeta) \cos\left(\frac{2\pi x}{L}\right) + \alpha_s(t; \zeta) \sin\left(\frac{2\pi x}{L}\right) \quad (4)$$

where $\alpha_c(t; \zeta)$ and $\alpha_s(t; \zeta)$ are uncorrelated Gaussian random variables with zero mean and standard deviation ζ . (*i.e.* white noise). The moment of the Froude-Krylov and hydrostatic forces can then be expressed as:

$$M_{FKHS}(\theta, t, \zeta) = \int_{-L/2}^{L/2} xA(x, \theta x + h(x, t; \zeta)) dx \quad (5)$$

For the description of the vertical bending moment, the model is limited to decoupled pitch in longitudinal waves without forward speed effect:

$$I\ddot{\theta} + c\dot{\theta} + M_{FKHS}(\theta, t, \zeta) = 0 \quad (6)$$

where $I = \int_{-L/2}^{L/2} x^2 m(x) dx$ is the moment of inertia and c is the damping coefficient.

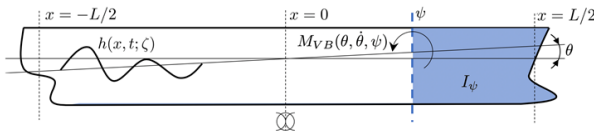


Figure 9: Derivation of an equation for the vertical bending moment at an arbitrary location along the length of the ship, ψ

Given the pitch motion, the VBM at an arbitrary point of the ship can be found. Referring to Figure 9, the following equation can be written for the vertical bending moment at an arbitrary location ψ :

$$I_\psi \ddot{\theta} + c_\psi \dot{\theta} + \int_{\psi}^{L/2} xA(x, \theta x + h) dx = M_{VB}(\theta, \dot{\theta}, \psi) \quad (7)$$

where

$$I_\psi = \int_{\psi}^{L/2} x^2 m(x) dx ; \quad c_\psi = \frac{c}{L} \left(\frac{L}{2} - \psi \right) \quad (8)$$

In the above expression for c_ψ , it is assumed that the hydrodynamic damping on each hull segment acts proportionally to its length. Solving equation (7) with respect to the pitch acceleration, $\ddot{\theta}$, and substituting into equation (5), an expression for the vertical bending moment at an arbitrary location of the ship can be obtained in terms of θ and $\dot{\theta}$.

APPROXIMATE VOLUME-BASED MODEL

In order to derive a distribution of the vertical bending moment, consider an expansion of the submerged area of a station around θx_i . Without imposing any constraints on the wave elevation h , one can write:

$$A(x, \theta x + h) = A(x, \theta x) + \sum_{q=1}^Q \frac{A^{(q)}(x, \theta x)}{q!} h^q \quad (9)$$

where Q is chosen according to the magnitude of h and how complicated the shape of $A(x, d)$ is. The superscript in parenthesis stands for the derivative of corresponding order.

Pitch motion is assumed to be Gaussian, as are its first and second derivatives. The terms $I_\psi \ddot{\theta}$ and $c_\psi \dot{\theta}$ then only contribute to the variance, but not to the shape of the distribution of VBM, and can thus be neglected in the present study.

An approximate formula for the vertical bending moment is expressed as:

$$M_{VB}(\theta, t, \zeta) = \int_{\psi}^{L/2} xA(x, \theta x) dx + \sum_{q=1}^Q \int_{\psi}^{L/2} xA^{(q)}(x, \theta x) \frac{h(x, t; \zeta)^q}{q!} dx \quad (10)$$

The first term is the vertical bending moment in calm water, when a ship is trimmed by the angle θ :

$$M_{VB0}(\theta, t, \zeta) = \int_{\psi}^{L/2} xA(x, \theta x) dx \quad (11)$$

The second term of the equation (9) expresses the influence of the random waves and pitch motion.

$$M_{VBW}(\theta, t, \zeta) = \sum_{q=1}^Q \int_{\psi}^{L/2} xA^{(q)}(x, \theta x) \frac{h(x, t; \zeta)^q}{q!} dx \quad (12)$$

Further analysis will rely on a second-order expansion, *i.e.* maintaining up to second-order interactions between waves. Following this set up, the vertical bending moment takes the form:

$$M_{VB}(\theta, t, \zeta) = \int_{\psi}^{L/2} xA(x, \theta x) dx + \int_{\psi}^{L/2} xA'(x, \theta x) h(x, t; \zeta) dx + \frac{1}{2} \int_{\psi}^{L/2} xA''(x, \theta x) h^2(x, t; \zeta) dx \quad (13)$$

For a fixed value of pitch angle θ :

$$M_{VB}(\theta, t, \zeta) \simeq \alpha_c(t; \zeta)\rho_c(\theta) + \alpha_s(t; \zeta)\rho_s(\theta) + 0.5\alpha_c^2(t; \zeta)\rho_{c2}(\theta) + 0.5\alpha_s^2(t; \zeta)\rho_{s2}(\theta) + \alpha_c(t; \zeta)\alpha_s(t; \zeta)\rho_{cs}(\theta) \quad (14)$$

where:

$$\begin{aligned} \rho_c(\theta) &= \int_{\psi}^{\frac{L}{2}} xA'(x, \theta x) \cos\left(\frac{2\pi x}{L}\right) dx \\ \rho_s(\theta) &= \int_{\psi}^{\frac{L}{2}} xA'(x, \theta x) \sin\left(\frac{2\pi x}{L}\right) dx \\ \rho_{c2}(\theta) &= \int_{\psi}^{\frac{L}{2}} xA''(x, \theta x) \cos^2\left(\frac{2\pi x}{L}\right) dx \\ \rho_{s2}(\theta) &= \int_{\psi}^{\frac{L}{2}} xA''(x, \theta x) \sin^2\left(\frac{2\pi x}{L}\right) dx \\ \rho_{cs}(\theta) &= \int_{\psi}^{\frac{L}{2}} xA''(x, \theta x) \cos\left(\frac{2\pi x}{L}\right) \sin\left(\frac{2\pi x}{L}\right) dx \end{aligned} \quad (15)$$

The model of VBM is still a function of pitch angle. The final hypothesis is that the VBM primarily depends on waves and the influence of the pitch angle is not essential. This hypothesis is implemented by averaging the function ρ using a Gaussian distribution and the variance of pitch σ_θ^2 estimated from the LAMP simulations:

$$\rho_{mc} = \frac{1}{\sigma_\theta\sqrt{2\pi}} \int_{-2\sigma_\theta}^{2\sigma_\theta} \rho_c(\theta) \exp\left(-\frac{\theta^2}{2\sigma_\theta^2}\right) d\theta \quad (16)$$

The values of ρ_{ms} , ρ_{mc2} , ρ_{ms2} and ρ_{mcs} are defined analogously to the above.

Finally, the approximate volume-based model for vertical bending moment is formulated as:

$$M_{VB}(t, \zeta) \simeq \alpha_c(t; \zeta)\rho_{mc} + \alpha_s(t; \zeta)\rho_{ms} + 0.5\alpha_c^2(t; \zeta)\rho_{mc2} + 0.5\alpha_s^2(t; \zeta)\rho_{ms2} + \alpha_c(t; \zeta)\alpha_s(t; \zeta)\rho_{mcs} \quad (17)$$

Formula (17) is intended to model the shape of the distribution and needs to be shifted to zero mean and normalized to unity variance. The standard deviation ζ of wave amplitudes α_c and α_s are meant to be fit from simulation or model data, perhaps using maximum likelihood estimator.

VBM DISTRIBUTION WITH APPROXIMATE VOLUME-BASED MODEL

Brown and Pipiras (2020) derived a theoretical PDF for the approximate volume-based model of VBM. It is expressed through the following integral:

$$f(\mu) = \frac{1}{2} \int_0^{2\pi} f_{2N}(\cos\varphi\sqrt{\mu - \mu_s}, \sin\varphi\sqrt{\mu - \mu_s}) d\varphi \quad (18)$$

where μ is vertical bending moment before shifting and normalization, and f_{2N} is a bivariate normal distribution. The value μ_s is computed as:

$$\mu_s = \frac{a_2^2 b_1 + a_1^2 b_2 - a_1 a_2 b_{12}}{4b_1 b_2 - b_{12}^2} \quad (19)$$

where

$$\begin{aligned} a_1 &= \rho_{mc}\zeta; & a_2 &= \rho_{ms}\zeta; \\ b_1 &= -\rho_{mc2} \frac{\zeta^2}{2}; & b_2 &= -\rho_{ms2} \frac{\zeta^2}{2}; \end{aligned} \quad (20)$$

$$b_{12} = -\rho_{mcs}\zeta^2$$

where ζ is the standard deviation of wave amplitudes α_c and α_s .

To compute bivariate normal distribution in equation (18), one needs two mean values E_1 and E_2 , two variances V_1 and V_2 , and a correlation coefficient r_{12} :

$$\begin{aligned} E_1 &= -\frac{a_2}{2\sqrt{b_2}} & E_2 &= \frac{a_2 b_{12} - 2a_1 b_2}{2\sqrt{b_2}\sqrt{4b_1 b_2 - b_{12}^2}} \\ V_1 &= \frac{b_{12}^2}{4b_2} - b_2 & V_2 &= \frac{4b_1 b_2 - b_{12}^2}{4b_2} \\ r_{12} &= \frac{b_{12}\sqrt{4b_1 b_2 - b_{12}^2}}{2b_2\sqrt{V_1 V_2}} \end{aligned} \quad (21)$$

There is a condition of applicability of the distribution:

$$4b_1 b_2 - b_{12}^2 > 0; \quad (22)$$

Also, μ_s has a meaning of a hogging limit; see Brown and Pipiras (2020) for more information.

To represent a shape, equation (16) needs to be shifted to zero mean and unity variance. To carry out this transformation, the actual values of mean and variance of the distribution (16) are computed

$$E_\mu = \int_{\mu_s}^{\infty} f(\mu)\mu d\mu \quad (23)$$

$$V_\mu = \int_{\mu_s}^{\infty} f(\mu)(\mu - E_\mu)^2 d\mu \quad (24)$$

Standard deviation is computed as:

$$\sigma_\mu = \sqrt{V_\mu} \quad (25)$$

The new variable is introduced:

$$y = \frac{\mu - E_\mu}{\sigma_\mu} \quad (26)$$

Finally the standardized PDF of vertical bending moment is expressed as:

$$pdf(y) = \sigma_\mu f(\sigma_\mu y + E_\mu) \quad (27)$$

NUMERICAL RESULTS FOR THE APPROXIMATE VOLUME-BASED MODEL

For the numerical implementation of the approximate volume-based model, the flared hull geometry (Figure 1) was represented by 100 stations, as shown in Figure 10. The submerged areas of the stations were computed with the trapezoid rule, and the first and second derivatives were computed for each point at each station. Linear interpolation was then used for computing the function ρ in equation (15).

The functions (15) were further averaged over pitch angles. The standard deviation for pitch angle was estimated using the results of the LAMP simulation for SS7, giving a value of $\hat{\sigma}_\theta = 2.4^\circ$. No significant difference in the standard deviation of the pitch motion was observed between the simulations with and without the deck pressures.

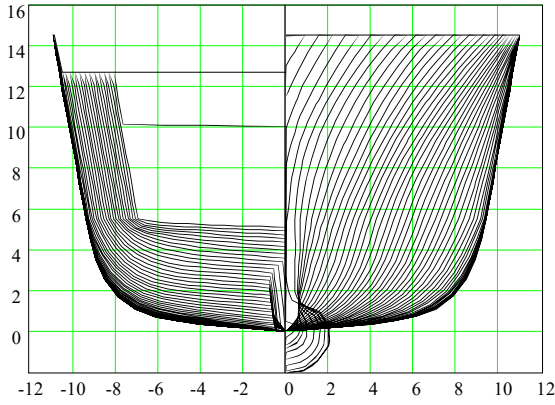


Figure 10: Station representation of ONR Topsides Series flared configuration

Table 2 Numerical Parameters for Approximate Volume-based Model of VBM in SS7

Standard deviation of wave amplitudes, ζ , m	4.73
Coefficient ρ_{mc} , N	-2,006.8
Coefficient ρ_{ms} , N	-13,189.1
Coefficient ρ_{mc2} , N/m	1065.1
Coefficient ρ_{ms2} , N/m	749.5
Coefficient ρ_{mcs} , N/m	552.8

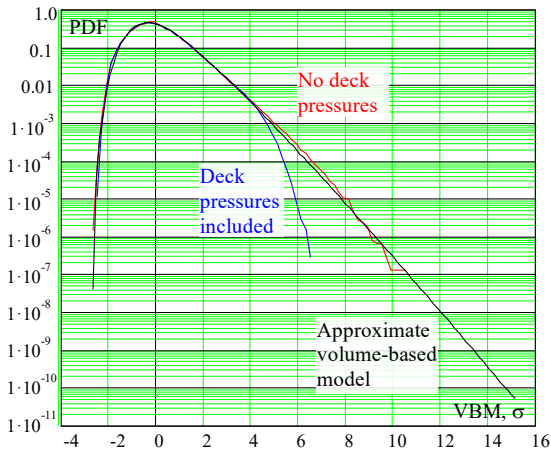


Figure 11: PDF of the approximated volume-based model in comparison with standardized histograms of VBM for SS7

Finally, the standard deviation of wave amplitude was found to achieve the best fit of the model. While some kind of maximum likelihood estimator is meant to be developed for future applications, the value in this example was found manually. This value, as well as the values of averaged ρ -functions, are given in Table 2. The resulting PDF is shown in Figure 11, where it is

compared with the standardized histogram of VBM from the simulations.

The standardization of the histograms for the instantaneous values of VBM (see Figure 4) was carried out using equation (27) with the mean and standard deviation of VBM estimated from the LAMP simulations.

ANALYSIS

The PDF of the approximate volume based model fits very well with the standardized histogram of VBM that did not include water on deck. The tail of the distribution of the volume-based model does not have any inflection point; so the approximate model is not expected to describe the effect of pressures on the deck.

The approximate volume-based model well describes the asymmetry of the distribution observed in histograms of instantaneous VBM values (Figure 4). Also, the topology of the PDF of the approximate volume based model is similar to the histogram of positive peaks of VBM (*i.e.* sagging peaks) shown in Figure 5.

The approximate volume-based model for vertical bending moment in form (17) includes wave influence explicitly, as modeled by equation (7). The influence of pitch motions is included implicitly, through averaging, resulting in equation (16). The influence of inertia and weight are not included, as these factors only affect the mean value and variance and do not affect the shape of the tail of the distribution.

These observations allow the formulation of the following hypothesis:

- Asymmetry of distribution of VBM is mostly related with wave action.
- The shape of the Weibull distribution may describe influences of wave passing a ship, while weight distribution, motions, and inertial forces mostly contribute to the mean and variance.
- Modeling of the inflection point may require more accurate modeling of motions, in particular, consideration of nonlinearity of the term:

$$\int_{\psi}^L x A(x, \theta x) dx. \text{ Heave motion may have to be included in order to get realistic waterlines.}$$

SUMMARY, CONCLUSIONS, AND FUTURE WORK

Large simulation datasets for vertical bending moment in head seas was produced with the Large Amplitude Motion Program (LAMP) for Sea States 5 and 7. Simulations for SS7 were carried out with and without deck pressures associated with the submergence of the ship's bow due to large relative motion, while SS5 included the deck pressures but saw few bow submergences. Inclusion of deck pressure reduces the VBM during deck submergences and leads to the

appearance of an inflection point in the histogram of VBM in SS7; no inflection point is observed for SS5. The VBM distribution in SS5 is similar to the distribution of VBM in SS 7 if the deck pressures are not included. The distribution of the sagging peaks behaved in a similar way: including deck pressures leads to the appearance of the inflection point, but only for SS7.

Weibull distribution provides a very good fit for SS5 and SS7 without deck pressures, but does not model the inflection point for the SS7 dataset including the deck pressure. If the reduction in VBM due to deck pressure can reasonably be included in the evaluation of the main girder loads, then an indiscriminant application of Weibull distribution may lead to significant overestimation of the VBM in high sea states if the position of the inflection point corresponds to the return period falling short of the desired lifetime.

A reduced-order probabilistic model was proposed for further study of the tail of the VBM with the intention of finding the location of the inflection point. The reduced order model uses a simplified presentation of irregular waves, containing two components of random amplitudes and wave length equal to the ship length. The model allows the influence of weight and inertia to be excluded, as they are believed to influence only the mean value and variance.

A further simplification of the model was achieved using a Taylor series expansion that allows the separation of the contribution of waves from the contribution of pitch motions. The approximated model compared very well with the simulation dataset that did not include deck pressure. This comparison has led to formulation of a hypothesis that the observed asymmetry, which is well described by the Weibull distribution, can be explained by the influence of waves.

The approximate model is capable of explaining the influence of waves on the vertical bending moment. It is similar to a Weibull distribution, but has a clear physical background. Making the approximate model into a working tool will require the development of robust fitting procedures and extensive testing.

The model needs to be extended to include the effect of pressure on the deck and a capability to reproduce the inflection point. The inflection point may play a role of an applicability limit of Weibull distribution to evaluate life-time wave loads. In a more general sense, the proper and consistent modeling of deck submergence events in the calculation of main-girder loads and the evaluation of extreme values must be considered.

ACKNOWLEDGEMENTS

The work described in this paper has been funded by the Office of Naval Research (ONR) under Dr. Woei-Min Lin. This research was also a part of the NSWCCD Independent Applied Research (IAR) program under Dr. Jack Price.

The participation of Prof. Sapsis was facilitated by the NSWCCD Summer Faculty Program, while the participation of Prof. Pipiras was facilitated by the NSWCCD Summer Faculty and Sabbatical Programs, both of which are also managed by Dr. Jack Price.

The authors are very grateful for the support that made this work possible.

REFERENCES

Belenky, V.L., "Piecewise linear approach to nonlinear ship dynamics," Contemporary Ideas on Ship Stability, Vassalos, D., Hamamoto, M., Papanikolaou, A., and Molyneux, D., eds., Elsevier, 2000, ISBN 0-08-043652-8, pp.149-160.

Belenky, V., Weems, K.M., Liut, D., and Shin, Y.S., "Nonlinear Roll with Water-on-Deck: Numerical Approach," Proceedings of the Eighth International Conference on the Stability of Ships and Ocean Vehicles (STAB 2003), Madrid, Spain, 2003.

Belenky, V., Weems, K., Pipiras, V., Glotzer, D., and Sapsis, T., "Tail Structure of Roll and Metric of Capsizing in Irregular Waves" Proceedings of the 32nd Symposium on Naval Hydrodynamics, Hamburg, Germany, 2018.

Belenky, V., Glotzer, D., Pipiras, V., and Sapsis, T., "Distribution tail structure and extreme value analysis of constrained piecewise linear oscillators", Probabilistic Engineering Mechanics, Vol. 57, 2019, pp 1-13.

Bishop, R.C., Belknap, W., Turner, C., Simon, B., and Kim, J.H., Parametric Investigation on the Influence of GM, Roll Damping, and Above-Water Form on the Roll Response of Model 5613, Carderock Division, Naval Surface Warfare Center Report NSWCCD-50-TR-2005/027, 2005.

Brown, B., and Pipiras, V., "Statistical Analysis of Extreme Ship Loads: Physical Distribution Tails, Limitations of Data-Driven Approaches and Model Uncertainty," Proceedings of the 33rd Symposium on Naval Hydrodynamics, Osaka, Japan, 2020.

Cohen, C.A., "Maximum Likelihood Estimation in the Weibull Distribution Based on Complete and On Censored Samples," Technometrics, Vol. 7, No. 4, Nov. 1965, pp. 579-588.

Liut, D., Weems, K.M., and Yen, T., "A Quasi-three-dimensional Finite-volume Shallow Water Model for Green Water on Deck," Journal of Ship Research, Vol. 57, No. 3, September 2013.

Ochi, M.K., and Wang, S., "Prediction of Extreme Wave-Induced Loads on Ocean Structures," Proceedings of the Symposium on Behavior of Offshore Structures, Vol. 1, 1976, pp. 170-186.

Ochi, M.K., "Principles of Extreme Value Statistics and their Application," Proceedings of the Extreme Loads Response Symposium, Society of Naval Architecture and Marine Engineering, Arlington, Virginia, USA, 1981, pp.15-30.

Shin, Y.S, Belenky, V.L., Lin, W.M., Weems, K.M., and Engle, A. H., "Nonlinear time domain simulation technology for seakeeping and wave-load analysis for modern ship design," Transactions, Society of Naval Architects and Marine Engineers, Vol. 111, 2003, pp. 557-578.

St. Denis, M., and Pierson, W.J., "On the Motion of Ships in Confused Seas," Transactions, Society of Naval Architects and Marine Engineers, Vol. 61, 1953.

Weems, K.M., Zhang, S., Lin, W.M, Bennet, J., and Shin, Y.S., "Structural Dynamic Loadings Due to Impact and Whipping," Seventh International Symposium on Practical Design of Ships and Mobile Units (PRADS98), The Hague, The Netherlands, 1998.